Responsive Materials

Deutsche Ausgabe: DOI: 10.1002/ange.201603030
Internationale Ausgabe: DOI: 10.1002/anie.201603030

Visualizing the Dynamics of Temperature- and Solvent-Responsive Soft Crystals

Jiandong Pang, Caiping Liu, Yougui Huang, Mingyan Wu, Feilong Jiang, Daqiang Yuan,* Falu Hu, Kongzhao Su, Guoliang Liu, and Maochun Hong*

Abstract: *We demonstrate that three flexible MOFs termed FJI-H11-R (FJI-H = Hong's group in Fujian Institute of Research on the Structure of Matter, R = Me, Et, ^{i}Pr) can reversibly respond to temperature and solvents via structural transformations, which can be visualized by in situ single-crystal X-ray snapshot analyses. FJI-H11-R exhibit colossal anisotropic thermal expansion, with a record-high uniaxial positive thermal-expansion coefficient of $653.2\times10^{-6}\ K^{-1}$ observed in FJI-H11-Me. Additionally, large c-axial shrinkage of 32.4% is also observed during desolvation. The stimuli-responsive mechanism reveals the structural evolutions are related to the rotations and deformations of the organic linkers.*

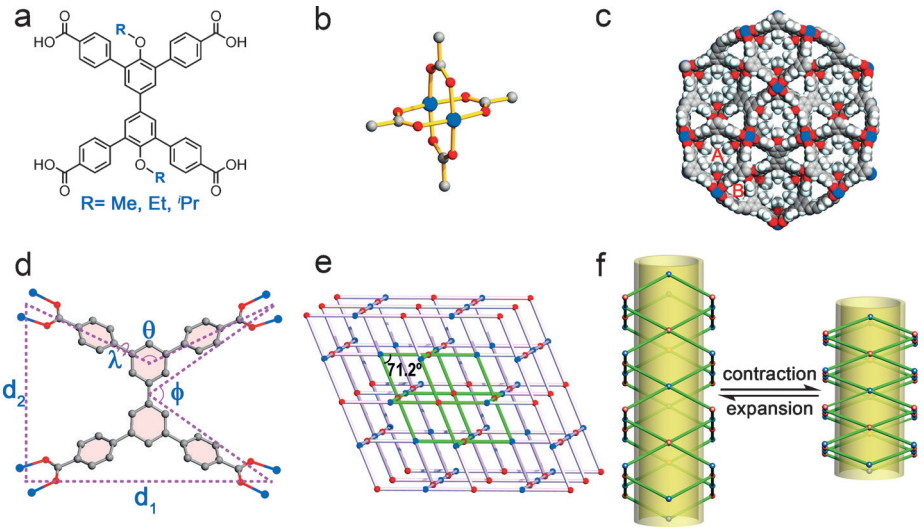

Figure 1. The crystal structure and topology of FJI-H11-R. a) The ligands. b) Cu^{II} SBU. Gray C, red O, blue Cu. c) Perspective view of the framework along the *c* axis. d) Definition of five parameters to estimate the rotation and distortion of the ligand: λ, d_1, d_2, θ, and φ. e) The distorted NbO-type topology with the angle of 71.2°. f) The illustration shows the hinged-framework motif responding to external stimuli.

In nature, the biomolecules can spontaneously respond to a specific stimulus or a subtle change in the local environments. To mimic nature, the design and engineering of artificial systems which can respond to external stimuli in a predictable and controllable manner is of great importance to the future intelligent technologies. These so-called "stimuli-responsive" or "smart" materials can undergo conformational changes or phase transitions in response to the external physical or chemical stimuli.[1] Among such "smart" materials, multi-stimuli-responsive materials are more important since their properties can be tuned by several different mechanisms, which act more similarly as natural macromolecules. Up to now, the explored dual/multi-stimuli-responsive systems are mainly on organic polymers, whose stimuli-responsive mechanism can't be visualized due to their non-crystalline nature.[2]

As unique hybrid crystalline materials, metal–organic frameworks (MOFs) have been widely investigated due to their potential applications especially in gas storage, separation, and sensing.[3] As proposed by Kitagawa and co-workers, the third generation materials are so-called flexible MOFs or soft porous crystals,[4] which can reversibly respond to external stimuli via a structural transition of the frameworks.[5] Furthermore, the tunable molecular design by modification of the organic ligands and the metal nodes will endow flexible MOFs with multiple functions, which is rarely seen in other solid-state materials.[6] More importantly, the mechanism of flexible MOFs responding to external stimulus can be visualized by X-ray diffractions, which may provide some insights to design new "smart" materials.[7]

Herein, we report a series of three-dimensional (3D) soft MOFs (FJI-H11-R), which are based on tetra-carboxylate ligands bearing dangling side groups (H_4L-R, Figure 1 a) and Cu^{II} paddle wheel secondary building units (SBUs). They can

[*] J. Pang, Dr. C. Liu, Prof. M. Wu, Prof. F. Jiang, Prof. D. Yuan, F. Hu, Dr. K. Su, G. Liu, Prof. M. Hong
State Key Lab of Structure Chemistry, Fujian Institute of Research on the Structure of Matter, CAS
Fuzhou, 350002, Fujian (China)
E-mail: wumy@fjirsm.ac.cn
ydq@fjirsm.ac.cn
J. Pang, F. Hu, G. Liu
University of Chinese Academy of Sciences
Beijing, 100049 (China)
Dr. Y. Huang
Institute for Materials Chemistry and Engineering, Kyushu University
Fukuoka, 8190395 (Japan)
Supporting information and the ORCID identification number(s) for the author(s) of this article can be found under http://dx.doi.org/10.1002/anie.201603030.

reversibly respond to temperature and solvents, which can be visualized by in situ single-crystal X-ray snapshot analyses.

Solvothermal reactions of H_4L-R (4,4′-di(substituent)oxybiphenyl-3,3′,5,5′-tetra-(phenyl-4-carboxylic acid)) with $Cu(NO_3)_2{\cdot}3H_2O$ in *N*,*N*-dimethylacetamide (DMA) afford the isoreticular framework complexes $[Cu_2(L\text{-}R)(H_2O)_2]_n{\cdot}(solvent)_x$ (FJI-H11-R, R = Me, Et, ^{i}Pr). Therefore, the ethyl substituted compound will be discussed in detail as a representative for brevity.

Single-crystal X-ray diffraction experiments at 293 K reveal FJI-H11-Et crystallizes in trigonal space group *R*-3m, which is constructed by fully deprotonated L-Et ligands and classical Cu^{II} SBUs. As expected, each Cu^{II} SBU links to four neighboring L-Et ligands and vice versa, resulting in two types of one-dimensional channels (A and B) along the crystallographic *c* axis (Figure 1c). On the wall of channel A, the L-Et ligand is obliquely arranged and the ethyl group of the L-Et ligand points into channel A. Interestingly, the dihedral angle of the inner biphenyl ring in L-Et ligand is close to zero, while the four outer benzoate groups are linked to the biphenyl core with a dihedral angle of 44.74°. For clarity, if we simplify both the ligands and the SBUs as planar 4-connected nodes, FJI-H11-Et possesses the (4,4)-c NbO-type network with the topological point symbol of $\{6^4.8^2\}$. Such 3D hinged-framework structure, which consists of two-dimensional rhombic fences, is well known for the great flexibility.[8] In FJI-H11-Et this NbO-type network is severely deformed with the angles of 71.2°, which is significantly deviated from the expected angle of 90°. Therefore, upon external stimuli the C–C bonds linking the phenyl rings may π-flip, which will lead to the compression or elongation of the channel A and B.

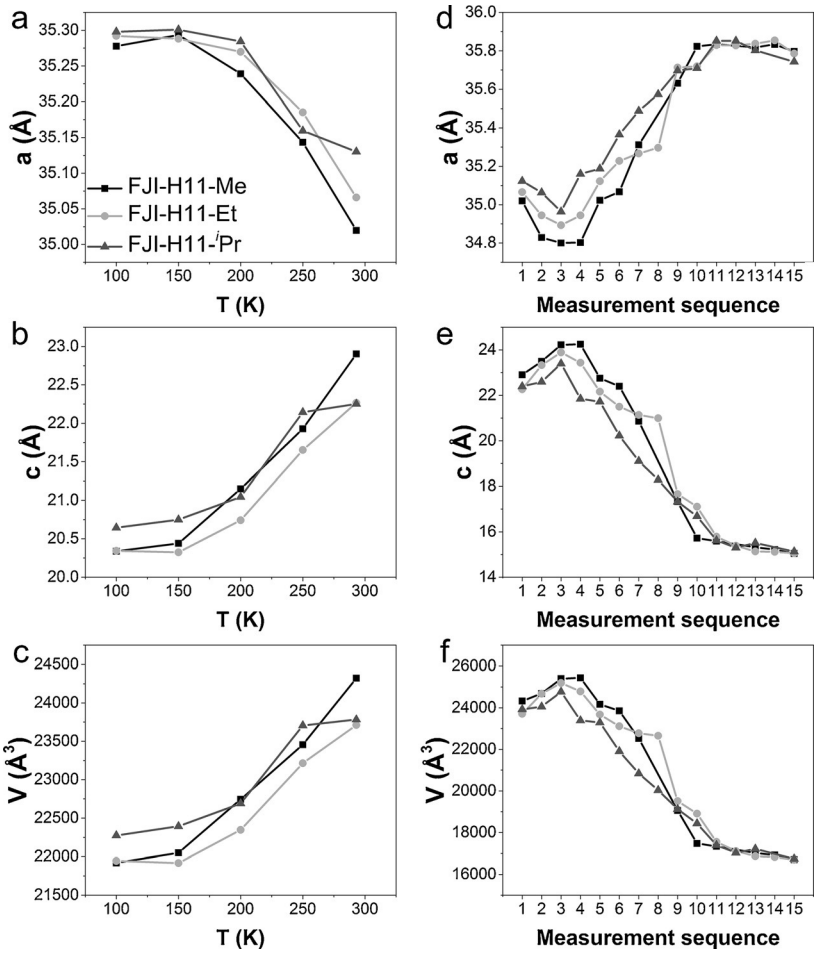

Figure 2. The changes of unit cell parameters during thermal expansion or desolvation for FJI-H11-R. The changes of *a* axis (a), *c* axis (b), and cell volume (c) during thermal expansion. During desolvation, the changes of *a* axis (d), *c* axis (e), and cell volume (f); the crystal data were collected at 293 K with intervals of 1 h, 5 h, and 24 h for measurement sequence 2– 5, 6–10, and 11–15, respectively. The error bars are apparently absent because of the very small errors.

Owning to the flexibility of such hinged-frameworks, they may respond to temperature stimulus. As anticipated, in situ variable-temperature single crystal X-ray diffraction experiments reveal FJI-H11-Et exhibits exceptional anisotropic thermal expansion property. From 100 K to 293 K, *a* axis exhibits a negative thermal expansion (NTE) with a slight decrease by 0.6%, but *c* axis has a positive thermal expansion (PTE) with a significant increase by 9.4%. Totally, the unit cell volume expands by 8.0% (Figure 2a–c). The average thermal expansion coefficients of FJI-H11-Et are $-33.2\times10^{-6}\,K^{-1}$, $489.4\times10^{-6}\,K^{-1}$, and $416.8\times10^{-6}\,K^{-1}$ for *a* axis, *c* axis and unit cell volume (*V*), respectively. Similar phenomena are observed in FJI-H11-Me and FJI-H11-^{i}Pr (Table 1). Especially, giant PTE coefficient of $653.2\times10^{-6}\,K^{-1}$ for the *c* axis is observed in FJI-H11-Me, which has greatly exceeded the previous record of $482.1\times10^{-6}\,K^{-1}$ for MOFs.[8d] These large thermal expansion coefficients are comparable to those reported for the organic polymer and thin film.[9] Notably, when cooled from 293 K to 100 K the unit cell parameters can recover, which indicates the reversibility of the thermal expansion.

Table 1: Temperature-dependent thermal expansion coefficients of FJI-H11-R[a].

R[b]	Δa[c]	α[d] [$\times10^{-6}\,K^{-1}$]	Δc	β [$\times10^{-6}\,K^{-1}$]	ΔV	γ [$\times10^{-6}\,K^{-1}$]
Me	−0.7%	−37.8(2)	12.6%	653.2(5)	11.0%	568.1(7)
Et	−0.6%	−33.2(3)	9.4%	489.4(10)	8.0%	416.8(11)
^{i}Pr	−0.5%	−24.6(2)	7.8%	403.7(4)	6.8%	350.8(5)

[a] FJI-H11-R remains in trigonal space group *R*-3 m. [b] Me, Et and ^{i}Pr are the abbreviation of FJI-H11-R (R = Me, Et, ^{i}Pr) respectively. [c] Δa, Δc, and ΔV represent variance ratio of the *a* axis, *c* axis, and cell volume, respectively. [d] α, β, and γ represent the thermal expansion coefficients of the *a* axis, *c* axis, and cell volume, respectively.

Single-crystal structures of FJI-H11-Et collected from 100 K to 293 K reveal the Cu–O bond lengths ($d_{Cu\text{-}O}$) and O-

Cu-O angles (ε) are almost unchanged, indicating the rigidity of the clusters. The dihedral angle between the Cu_2–O_2 plane and the carboxylate group $O_2>C$ (κ) increase from 0.40° to 1.32°, while the dihedral angle λ (Figure 1 d) decreases from 46.52° to 44.74° owing to π-flipping. To estimate the distortion of L-Et ligand, we have defined another four parameters, that is, d_1, d_2, θ, and φ. As shown in Figure 3, d_1 and θ decrease slightly from 17.65 Å and 131.51° to 17.53 Å and 129.57° respectively, leading to the decrease of the *a* and *b* axes. In contrast, d_2 and φ increase slightly from 12.24 Å and 69.49° to 12.55 Å and 71.20° respectively, causing the increase of the *c* axis. The manifest changes of d_1, θ, d_2 and φ indicate the L-Et ligand is distinctly bent.[6b,10] On the whole, colossal thermal expansions correlate strongly with the rotation and deformation of the L-Et ligand.

The flexible nature of FJI-H11-Et prompts us to investigate its dynamic feature in response to solvent molecules.[11] Exposing single crystal of FJI-H11-Et to the air at ambient condition, time-resolved single-crystal X-ray diffraction data were collected for 15 times over 150 h. With the solvent molecules gradually escaping, the unit cell parameters dramatically change (Figure 2 d–f) while the space group and the topology are retained. The *c* axis and *V* significantly contract from 22.27 Å and 23710 Å^3 to 15.06 Å and 16700 Å^3 respectively, while the *a* axis slightly expands from 35.07 Å to 35.79 Å concomitantly. The coefficients of expansion for *a*, *c*, and *V* are 2.1%, −32.4%, and −29.6%, respectively. Careful analysis of desolvated structures reveals the mechanism of the solvent response is similar to that of thermal expansion (Figure 4). Interestingly, the contraction or expansion is not monotonic. Initially, an abnormal contraction for *a* axis but an expansion for *c* axis and *V* are observed, which has not been reported previously. However, similar phenomena are also observed for FJI-H11-Me and FJI-H11-^{i}Pr. We infer these soft materials contract at *a* and *b* axes to diminish the channel size so as to prevent the escape of solvent molecules.

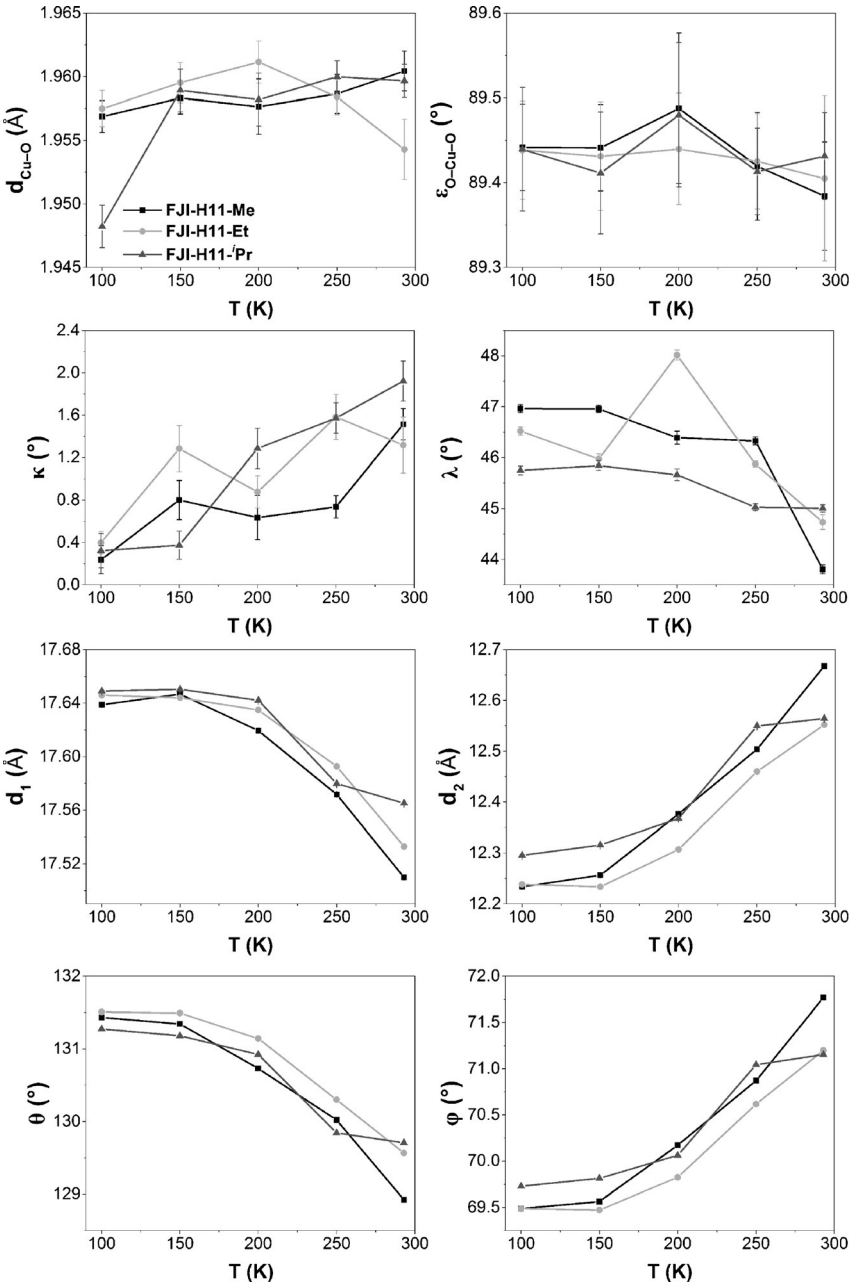

Figure 3. Temperature-dependent parameters of $d_{Cu\text{-}O}$, ε, κ, λ, d_1, d_2, θ,and φ for FJI-H11-R during thermal expansions. The error bars are apparently absent for some of the parameters because of the very small errors.

Desolvated samples of FJI-H11-Et are both directly exposed to DMA vapor under ambient condition. The regained PXRD patterns match with the as-synthesized ones, indicating the framework recovers upon absorbing DMA molecules (Figure S8). Fortunately, single crystal data of the regained FJI-H11-Et can also be obtained, which is almost the same as that of the as-synthesized one. Furthermore, the desolvated FJI-H11-Et can also respond to other solvents, such as DMF, DEF, methanol and 1,4-dioxane. The *V* expansion coefficients range from 33.3% to 59.7% following the sequence of DEF > 1,4-dioxane > DMF > DMA > methanol (Table S10 and Table S12), which is related to the polarity and size of the guest molecules (nonpolar > polar, large molecular size > small molecular size).[6b,11a]

Cramb, Shimizu, and co-workers have reported an example of multi-step single-crystal-to-single-crystal transformations on dehydration.[12] Though two partially dehydrated transition phases are detected, other successive intermediates

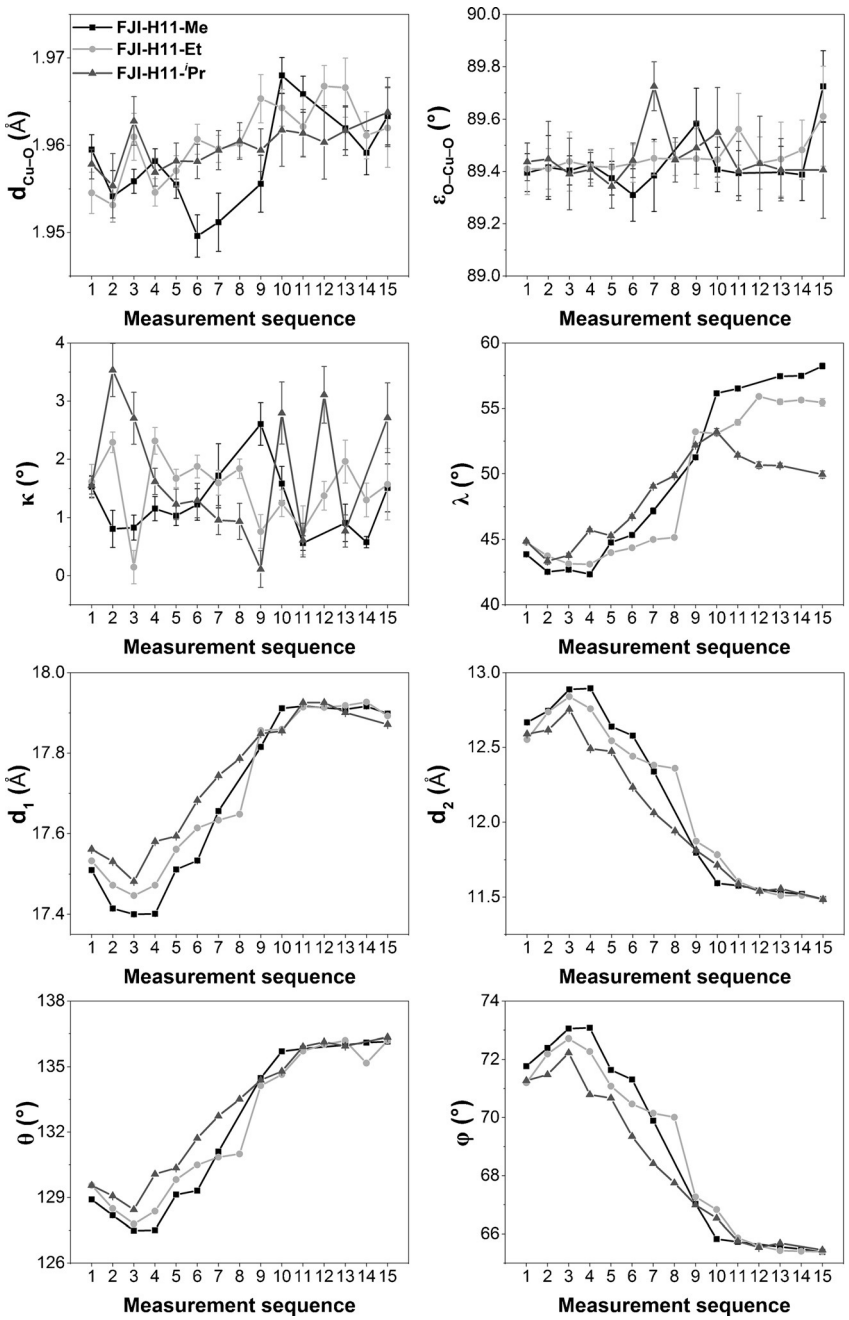

Figure 4. The parameters of $d_{Cu\text{-}O}$, ε, κ, λ, d_1, d_2, θ, and φ for FJI-H11-R during desolvation. The error bars are apparently absent for some of the parameters because of the very small errors.

can only give the unit cells due to the severe statistics. In comparison, the desolvation process of FJI-H11-R is unique. The snapshots of the successive intermediate states are achieved upon desolvation and their structures are unambiguously solved, which present more precise pictures of the mechanism of the dynamic behavior (Figure 5).

As a kind of neutral molecules, gases may also be used as stimuli to FJI-H11-Et. N_2 sorption isotherm at 77 K indicates an obvious breathing behavior (Figure S9). Small amount of N_2 is absorbed in the low-pressure region but an abrupt increase is observed above 570 mbar. Additionally, a pronounced hysteresis is observed, which suggests the adsorption occurs with the structural transformations. Similar phenomena can also be observed for FJI-H11-Me and FJI-H11-^{i}Pr.

In summary, we have reported a series of soft crystal materials, which show interesting dynamic features in response to thermal treatment and solvent molecules as a result of the rotation and bending of the organic linkers. Importantly, the successive intermediate states of both thermal expansion and desolvation can be visualized by in situ X-ray snapshot analyses, which bring us a closer inspection of the stimuli-responsive mechanisms. It is much helpful to us for the design and syntheses of these "smart" materials. Further research is undergoing in our group.

Acknowledgements

This work was financially supported by NSFC (21131006, 21271172, and 21371169), 973 Program (2014CB932101 and 2013CB933200), and Youth Innovation Promotion Association CAS. We thank Prof. Lin-Bing Sun for his contributions on materials characterization.

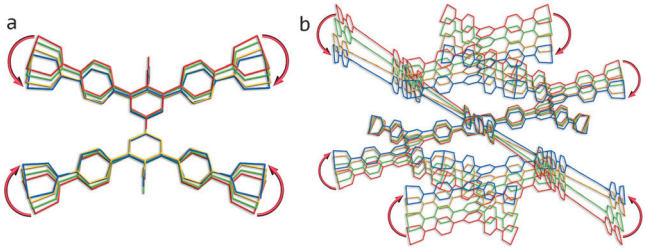

Figure 5. Changes of the organic ligand and the framework in FJI-H11-Et during desolvation. a) The overlay of organic ligand. b) The overlay of crystal structure along the [010] direction. The direction arrow indicate the shrinking trend of the frameworks during desolvation.

Keywords: metal–organic frameworks · solvent responsive · stimuli-responsive materials · temperature responsive · X-ray snapshot analyses

How to cite: *Angew. Chem. Int. Ed.* **2016**, *55*, 7478–7482
Angew. Chem. **2016**, *128*, 7604–7608

[1] a) J. Rabone, Y. F. Yue, S. Y. Chong, K. C. Stylianou, J. Bacsa, D. Bradshaw, G. R. Darling, N. G. Berry, Y. Z. Khimyak, A. Y. Ganin, P. Wiper, J. B. Claridge, M. J. Rosseinsky, *Science* **2010**, *329*, 1053; b) A. B. Cairns, J. Catafesta, C. Levelut, J. Rouquette, A. van der Lee, L. Peters, A. L. Thompson, V. Dmitriev, J. Haines, A. L. Goodwin, *Nat. Mater.* **2013**, *12*, 212; c) D. Liu, T. F.

Liu, Y. P. Chen, L. Zou, D. Feng, K. Wang, Q. Zhang, S. Yuan, C. Zhong, H. C. Zhou, *J. Am. Chem. Soc.* **2015**, *137*, 7740; d) W. Cai, A. Gladysiak, M. Aniola, V. J. Smith, L. J. Barbour, A. Katrusiak, *J. Am. Chem. Soc.* **2015**, *137*, 9296; e) J. Sotelo, C. H. Woodall, D. R. Allan, E. Gregoryanz, R. T. Howie, K. V. Kamenev, M. R. Probert, P. A. Wright, S. A. Moggach, *Angew. Chem. Int. Ed.* **2015**, *54*, 13332; *Angew. Chem.* **2015**, *127*, 13530; f) A. U. Ortiz, A. Boutin, K. J. Gagnon, A. Clearfield, F. X. Coudert, *J. Am. Chem. Soc.* **2014**, *136*, 11540.

[2] a) S. Guragain, B. P. Bastakoti, V. Malgras, K. Nakashima, Y. Yamauchi, *Chem. Eur. J.* **2015**, *21*, 13164; b) F. D. Jochum, P. Theato, *Chem. Soc. Rev.* **2013**, *42*, 7468; c) P. K. Kundu, G. L. Olsen, V. Kiss, R. Klajn, *Nat. Commun.* **2014**, *5*, 3588.

[3] a) J. R. Li, J. Sculley, H. C. Zhou, *Chem. Rev.* **2012**, *112*, 869; b) H. Sung Cho, H. Deng, K. Miyasaka, Z. Dong, M. Cho, A. V. Neimark, J. Ku Kang, O. M. Yaghi, O. Terasaki, *Nature* **2015**, *527*, 503; c) A. Douvali, A. C. Tsipis, S. V. Eliseeva, S. Petoud, G. S. Papaefstathiou, C. D. Malliakas, I. Papadas, G. S. Armatas, I. Margiolaki, M. G. Kanatzidis, T. Lazarides, M. J. Manos, *Angew. Chem. Int. Ed.* **2015**, *54*, 1651; *Angew. Chem.* **2015**, *127*, 1671.

[4] a) S. Horike, S. Shimomura, S. Kitagawa, *Nat. Chem.* **2009**, *1*, 695; b) S. Shimomura, M. Higuchi, R. Matsuda, K. Yoneda, Y. Hijikata, Y. Kubota, Y. Mita, J. Kim, M. Takata, S. Kitagawa, *Nat. Chem.* **2010**, *2*, 633.

[5] a) G. Ferey, C. Serre, *Chem. Soc. Rev.* **2009**, *38*, 1380; b) Y. Sakata, S. Furukawa, M. Kondo, K. Hirai, N. Horike, Y. Takashima, H. Uehara, N. Louvain, M. Meilikhov, T. Tsuruoka, S. Isoda, W. Kosaka, O. Sakata, S. Kitagawa, *Science* **2013**, *339*, 193; c) M. Zhu, X.-Z. Song, S.-Y. Song, S.-N. Zhao, X. Meng, L.-L. Wu, C. Wang, H.-J. Zhang, *Adv. Sci.* **2015**, *2*, 1500012.

[6] a) S. Henke, A. Schneemann, A. Wutscher, R. A. Fischer, *J. Am. Chem. Soc.* **2012**, *134*, 9464; b) Y. S. Wei, K. J. Chen, P. Q. Liao, B. Y. Zhu, R. B. Lin, H. L. Zhou, B. Y. Wang, W. Xue, J. P. Zhang, X. M. Chen, *Chem. Sci.* **2013**, *4*, 1539; c) Z. Chang, D. H. Yang, J. Xu, T. L. Hu, X. H. Bu, *Adv. Mater.* **2015**, *27*, 5432; d) A. Schneemann, V. Bon, I. Schwedler, I. Senkovska, S. Kaskel, R. A. Fischer, *Chem. Soc. Rev.* **2014**, *43*, 6062; e) D. Dubbeldam, K. S. Walton, D. E. Ellis, R. Q. Snurr, *Angew. Chem. Int. Ed.* **2007**, *46*, 4496; *Angew. Chem.* **2007**, *119*, 4580.

[7] a) J. P. Zhang, P. Q. Liao, H. L. Zhou, R. B. Lin, X. M. Chen, *Chem. Soc. Rev.* **2014**, *43*, 5789; b) F.-X. Coudert, *Chem. Mater.* **2015**, *27*, 1905; c) S. S. Nagarkar, A. V. Desai, S. K. Ghosh, *Chem. Asian J.* **2014**, *9*, 2358; d) A. J. McConnell, C. S. Wood, P. P. Neelakandan, J. R. Nitschke, *Chem. Rev.* **2015**, *115*, 7729; e) H. L. Zhou, R. B. Lin, C. T. He, Y. B. Zhang, N. Feng, Q. Wang, F. Deng, J. P. Zhang, X. M. Chen, *Nat. Commun.* **2013**, *4*, 2534; f) S. G. Duyker, V. K. Peterson, G. J. Kearley, A. J. Ramirez-Cuesta, C. J. Kepert, *Angew. Chem. Int. Ed.* **2013**, *52*, 5266; *Angew. Chem.* **2013**, *125*, 5374; g) T. Jacobs, G. O. Lloyd, J. A. Gertenbach, K. K. Muller-Nedebock, C. Esterhuysen, L. J. Barbour, *Angew. Chem. Int. Ed.* **2012**, *51*, 4913; *Angew. Chem.* **2012**, *124*, 4997; h) J. Marti-Rujas, M. Kawano, *Acc. Chem. Res.* **2013**, *46*, 493; i) W. M. Bloch, A. Burgun, C. J. Coghlan, R. Lee, M. L. Coote, C. J. Doonan, C. J. Sumby, *Nat. Chem.* **2014**, *6*, 906.

[8] a) G. B. Gardner, D. Venkataraman, J. S. Moore, S. Lee, *Nature* **1995**, *374*, 792; b) A. Galet, V. Niel, M. C. Munoz, J. A. Real, *J. Am. Chem. Soc.* **2003**, *125*, 14224; c) L. D. DeVries, P. M. Barron, E. P. Hurley, C. Hu, W. Choe, *J. Am. Chem. Soc.* **2011**, *133*, 14848; d) H. L. Zhou, Y. B. Zhang, J. P. Zhang, X. M. Chen, *Nat. Commun.* **2015**, *6*, 6917; e) W. Cai, A. Katrusiak, *Nat. Commun.* **2014**, *5*, 4337; f) B. Manna, A. K. Chaudhari, B. Joarder, A. Karmakar, S. K. Ghosh, *Angew. Chem. Int. Ed.* **2013**, *52*, 998; *Angew. Chem.* **2013**, *125*, 1032.

[9] a) E. Gann, X. K. Gao, C. A. Di, C. R. McNeill, *Adv. Funct. Mater.* **2014**, *24*, 7211; b) X. Shen, C. Viney, E. R. Johnson, C. Wang, J. Q. Lu, *Nat. Chem.* **2013**, *5*, 1035.

[10] P. Deria, D. A. Gomez-Gualdron, W. Bury, H. T. Schaef, T. C. Wang, P. K. Thallapally, A. A. Sarjeant, R. Q. Snurr, J. T. Hupp, O. K. Farha, *J. Am. Chem. Soc.* **2015**, *137*, 13183.

[11] a) C. Serre, C. Mellot-Draznieks, S. Surble, N. Audebrand, Y. Filinchuk, G. Ferey, *Science* **2007**, *315*, 1828; b) P. K. Allan, B. Xiao, S. J. Teat, J. W. Knight, R. E. Morris, *J. Am. Chem. Soc.* **2010**, *132*, 3605; c) C. Shi, X. Zhang, Y. Cai, Y. F. Yao, W. Zhang, *Angew. Chem. Int. Ed.* **2015**, *54*, 6206; *Angew. Chem.* **2015**, *127*, 6304; d) F. Millange, N. Guillou, M. E. Medina, G. r. Férey, A. Carlin-Sinclair, K. M. Golden, R. I. Walton, *Chem. Mater.* **2010**, *22*, 4237; e) S. Henke, W. Li, A. K. Cheetham, *Chem. Sci.* **2014**, *5*, 2392.

[12] B. D. Chandler, G. D. Enright, K. A. Udachin, S. Pawsey, J. A. Ripmeester, D. T. Cramb, G. K. Shimizu, *Nat. Mater.* **2008**, *7*, 229.

Received: March 28, 2016
Published online: May 4, 2016

